doi:10.1016/j.jmb.2009.03.068 J. Mol. Biol. (2009) 389, 275–288

JMB

Available online at www.sciencedirect.com

ScienceDirect

ELSEVIER

Kinetic Analysis of the Guanine Nucleotide Exchange Activity of TRAPP, a Multimeric Ypt1p Exchange Factor

Harvey F. Chin[1], Yiying Cai[2], Shekar Menon[3], Susan Ferro-Novick[3], Karin M. Reinisch[2] and Enrique M. De La Cruz[1]*

[1]*Department of Molecular Biophysics and Biochemistry, Yale University, PO Box 208114, 260 Whitney Avenue, New Haven, CT 06520-8114, USA*

[2]*Department of Cell Biology, Yale University School of Medicine, 333 Cedar Street, New Haven, CT 06520, USA*

[3]*The Howard Hughes Medical Institute and the Department of Cellular and Molecular Medicine, University of California at San Diego, La Jolla, CA 92093-0668, USA*

Received 23 January 2009; received in revised form 24 March 2009; accepted 30 March 2009
Available online 8 April 2009

Edited by J. Karn

TRAPP complexes, which are large multimeric assemblies that function in membrane traffic, are guanine nucleotide exchange factors (GEFs) that activate the Rab GTPase Ypt1p. Here we measured rate and equilibrium constants that define the interaction of Ypt1p with guanine nucleotide (guanosine 5′-diphosphate and guanosine 5′-triphosphate/guanosine 5′-(β,γ-imido)triphosphate) and the core TRAPP subunits required for GEF activity. These parameters allowed us to identify the kinetic and thermodynamic bases by which TRAPP catalyzes nucleotide exchange from Ypt1p. Nucleotide dissociation from Ypt1p is slow ($\sim 10^{-4}$ s^{-1}) and accelerated >1000-fold by TRAPP. Acceleration of nucleotide exchange by TRAPP occurs via a predominantly Mg^{2+}-independent pathway. Thermodynamic linkage analysis indicates that TRAPP weakens nucleotide affinity by <80-fold and vice versa, in contrast to most other characterized GEF systems that weaken nucleotide binding affinities by 4–6 orders of magnitude. The overall net changes in nucleotide binding affinities are small because TRAPP accelerates both nucleotide binding and dissociation from Ypt1p. Weak thermodynamic coupling allows TRAPP, Ypt1p, and nucleotide to exist as a stable ternary complex, analogous to strain-sensing cytoskeleton motors. These results illustrate a novel strategy of guanine nucleotide exchange by TRAPP that is particularly suited for a multifunctional GEF involved in membrane traffic.

© 2009 Elsevier Ltd. All rights reserved.

Keywords: GTPase; GEF; nucleotide exchange; vesicle trafficking; kinetics

Introduction

Small GTPase proteins of the Ras superfamily are chemical switches that regulate diverse cell biological processes ranging from vesicle trafficking and nuclear transport to signaling pathways.[1] Ras with bound guanosine 5′-triphosphate (GTP) activates downstream effector proteins and is inactive when guanosine 5′-diphosphate (GDP) is bound. The intrinsic rate of GDP dissociation ($t_{1/2}$>100 min) is extremely slow; *in vivo*, Ras GTPases are activated by guanine nucleotide exchange factors (GEFs), which accelerate this step. Intracellular nucleotide concentrations, where GTP concentrations are 10 times higher, then favor exchange of bound GDP for GTP. A number of GEFs have now been characterized both structurally and biochemically. Although structurally diverse, they use the same general strategy for accelerating nucleotide exchange. GEF activity is driven by allosteric competition between GEF binding and GDP binding that results in GDP affinity that is weakened 10^4–10^6 times by GEF binding.[2]

Members of the Rab subfamily of Ras GTPases play critical roles in regulating vesicle traffic between membrane-bound compartments.[3,4] A vesicle carrying cargo buds from the donor compartment and travels to a specific target compartment, where it is recognized and then fuses to deliver its cargo. Each trafficking pathway involves numerous protein components, including Rab proteins and large

*Corresponding author. E-mail address: enrique.delacruz@yale.edu.

Abbreviations used: GEF, guanine nucleotide exchange factor; GTP, guanosine 5c-triphosphate; GDP, guanosine 5c-diphosphate; mant, *N*-methylanthraniloyl; mant-dGDP, 2′-deoxy mantGDP; EDTA, ethylenediaminetetraacetic acid.

0022-2836/$ - see front matter © 2009 Elsevier Ltd. All rights reserved.

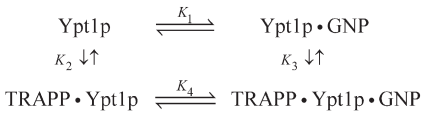
multisubunit tethering complexes. These complexes tether transport vesicles to their target compartment as the vesicle is recognized at the target membrane.[5]

In the yeast *Saccharomyces cerevisiae*, the Rab Ypt1p is involved in regulating vesicle transport to the Golgi apparatus. Ypt1p is activated by a large multisubunit complex called TRAPP that also functions in tethering.[5] TRAPP is found in two forms:[6] TRAPP-I mediates traffic from the endoplasmic reticulum to the early Golgi apparatus, while TRAPP-II plays a role in transport to the late Golgi apparatus.[7,8] The two TRAPP complexes share seven subunits (Bet3p, Bet5p, Trs31p, Trs33p, Trs23p, Trs20p, and Trs85p), of which four (Bet3p, Bet5p, Trs23p, and Trs31p) are required for activation of Ypt1p.[8,9] TRAPP is thus an unusual GEF in that its activity does not reside in a single subunit but instead requires a minimal five-subunit subcomplex comprising four different proteins.

We recently described the crystal structure of nucleotide-free Ypt1p bound to a TRAPP subcomplex that is minimally needed to activate Ypt1p.[10] A concurrent preliminary kinetic analysis of GTP binding and GDP exchange from wild-type and mutant TRAPP suggested that the acceleration of nucleotide exchange from Ypt1p by TRAPP occurs through a strategy distinct from those of other characterized GEFs. In this study, we perform a complete kinetic and equilibrium analysis of the interaction of Ypt1p with TRAPP and guanine nucleotides. We also determine the Mg^{2+} dependence of TRAPP GEF activity, which suggests an exchange mechanism occurring independent of Mg^{2+} displacement. Our results and analysis indicate that TRAPP functions differently from the majority of characterized GEFs in that allosteric weakening of GDP affinity does not completely account for activation. The kinetic and thermodynamic adaptations of TRAPP are suited for a multifunctional GEF involved in vesicle tethering.

Results

The interaction of Ypt1p with guanine nucleotides (GDP or GTP) and TRAPP, as with other GTPases and exchange factors,[2] is defined by the closed cyclic reaction scheme of linked equilibria presented in Scheme 1:



Scheme 1. Thermodynamic cycle for Ypt1p interactions with TRAPP and nucleotide.

where GNP represents either GDP or GTP, and K_i represents the overall dissociation equilibrium constants for binding of a given ligand. The results in the following sections are discussed in terms of this scheme, which has been used in characterizing other exchange factors.[2,11]

We measured guanine nucleotide (GTP, GDP, and guanosine 5′-(β,γ-imido)triphosphate) binding to Ypt1p (K_1 and K_4) using fluorescently modified *N*-methylanthraniloyl (mant) analogs. Previous measurements demonstrate that the mant fluorophore has negligible effects on Ypt1p nucleotide binding kinetics and affinity, and that mant–nucleotide analogs can be used to reliably measure guanine nucleotide binding to Ypt1p and related GTPases.[11,12]

TRAPP activation of mantGDP dissociation from Ypt1p

TRAPP activates Ypt1p under *in vivo* conditions by accelerating the exchange of bound GDP for free cytosolic GTP. We measured TRAPP-catalyzed dissociation of bound mantGDP from Ypt1p by monitoring reduction in fluorescence intensity after mixing an equilibrated mixture of Ypt1p and mantGDP (i.e., high-fluorescence Ypt1p–mantGDP

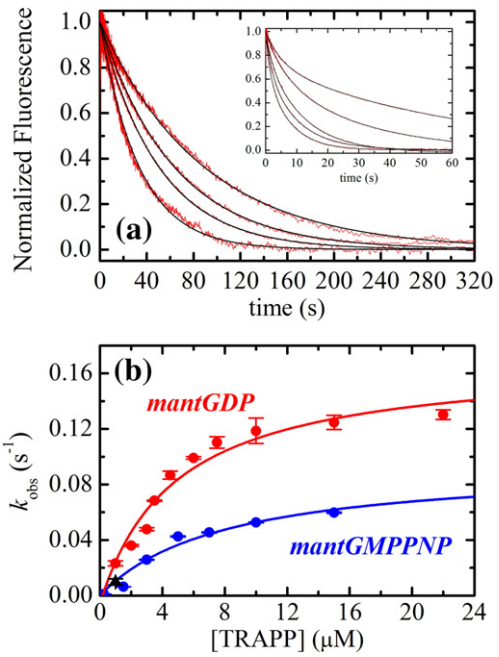


Fig. 1. TRAPP activation of nucleotide exchange from Ypt1p. (a) Time courses of mant-dGDP dissociation from 0.25 μM Ypt1p in the presence of (right to left) 1 μM, 1.5 μM, 2 μM, or 2.5 μM TRAPP. Inset: Time courses of mantGDP dissociation from 0.25 μM Ypt1p in the presence of (right to left) 1 μM, 3 μM, 4.5 μM, 6 μM, or 15 μM TRAPP. The smooth black lines through the data (red) represent the best fits to single (panel) or double (inset) exponentials. (b) [TRAPP] dependence of the observed rate constant for nucleotide dissociation. The smooth line is the best fit of the data to Eq. (1), with $k_{-4}=0.17\ s^{-1}$ and $K_3=4.8$ μM for mantGDP (red), and $k_{-4}=0.095\ s^{-1}$ and $K_3=8$ μM for mantGMPPNP dissociation (blue). The dissociation of [^{3}H]GDP from Ypt1p in the presence of 1 μM TRAPP is shown as a black triangle.

complex) with excess unlabelled GDP or GTP[13] and a range of [TRAPP]. Time courses of irreversible mantGDP dissociation from Ypt1p (in the presence of TRAPP) follow double exponentials, with a slow phase that dominates the transient and a fast phase that comprises ~10% of the total amplitude (Fig. 1a, inset). We interpret the fluorescence changes to reflect nucleotide dissociation. In support of this interpretation, dissociation of radiolabeled GDP from Ypt1p, as measured by filter binding,[10] yielded comparable (within a factor of 2) observed rate constants as fluorescence (Fig. 1b). We do not consider the possibility that a fluorescence change arises from fast TRAPP binding to Ypt1p–mantGDP because there is no fluorescence change upon mixing Ypt1p–mantGDP with TRAPP in the presence of excess mantGDP (data not shown), a condition in which mantGDP dissociation does not occur.

MantGDP exists as an equilibrium mixture of 2′- and 3′-labeled isomers, and the observed double-exponential time courses could arise from different dissociation kinetics of the two isomers. We therefore measured the exchange of a single isomer, 2′-deoxy mantGDP (mant-dGDP), from Ypt1p. Time courses of mant-dGDP dissociation from Ypt1p follow single exponentials (Fig. 1a), with observed rate constants (k_{obs}) comparable to the slow phase of mantGDP dissociation (Fig. 1a), consistent with the interpretation that the biphasic time courses result from differential binding of the mixed 2′ and 3′ isomers. We therefore focus our analysis and discussion of mantGDP to the predominant slow phase that comprises ~90% of the fluorescence transient.

The observed rate constants for irreversible mant-dGDP and mantGDP dissociation depend hyperbolically on [TRAPP] (Fig. 1b), indicating a two-step scheme for the acceleration of nucleotide exchange from Ypt1p by TRAPP, in which TRAPP binding to Ypt1p–GDP (K_3) is treated as a rapid equilibrium because it equilibrates more rapidly than GDP dissociates, as shown in Scheme 2:

$$\begin{array}{ccccc} \text{Ypt1p} \cdot \text{GDP} & \overset{K_3}{\rightleftharpoons} & \text{TRAPP} \cdot \text{Ypt1p} \cdot \text{GDP} & \xrightarrow{k_{-4}} & \text{TRAPP} \cdot \text{Ypt1p} + \text{GDP} \\ k_{-1}\downarrow & & & & \\ \text{Ypt1p} + \text{GDP} & & & & \end{array}$$

Scheme 2. Reaction scheme for acceleration of GDP dissociation from Ypt1p by TRAPP.

According to this scheme, the [TRAPP] dependence of k_{obs} is given by:

$$k_{obs} = \frac{(k_{-4} - k_{-1})[\text{TRAPP}]}{K_3 + [\text{TRAPP}]} + k_{-1} \qquad (1)$$

The best fit of the data to Eq. (1) yields a rate constant of 0.17 s^{-1} for GDP dissociation from the Ypt1p–TRAPP complex (k_{-4}) and an affinity of

Table 1. Rate and equilibrium constants for TRAPP and nucleotide binding to Ypt1p

$$\begin{array}{ccc} \text{Ypt1p} & \overset{K_1}{\rightleftharpoons} & \text{Ypt1p} \bullet \text{GNP} \\ K_2\downarrow\uparrow & & K_3\downarrow\uparrow \\ \text{TRAPP} \bullet \text{Ypt1p} & \overset{K_4}{\rightleftharpoons} & \text{TRAPP} \bullet \text{Ypt1p} \bullet \text{GNP} \end{array}$$

Parameter	Value	Source
GDP		
k_{+1}	0.096(±0.004) μM^{-1} s^{-1}	mant-dGDP binding
	0.05(±0.01) μM^{-1} s^{-1}	mantGDP binding[10]
k_{-1}	0.00012(±0.00002) s^{-1}	[^{3}H]GDP filter binding[10]
K_1	1.2(±0.2) nM	Ratio of rate constants
K_3	4.8(±1.2) μM	mantGDP/mant-dGDP (Fig. 1)
k_{+4A}	2.4(±0.1) μM^{-1} s^{-1}	Linear fit (Fig. 2)
	2.5(±0.1) μM^{-1} s^{-1}	Global fit (Fig. 2)
k_{-4A}	22.1(±2.0) s^{-1}	Linear fit (Fig. 2)
	15.7(±5.3) s^{-1}	Global fit (Fig. 2)
k_{+4B}	20.7(±2.2) s^{-1}	Hyperbolic fit (Fig. 2)
	11.7(±12.0) s^{-1}	Global fit (Fig. 2)
k_{-4B}	0.17(±0.01) s^{-1}	mantGDP/mant-dGDP (Fig. 1)
$K_{4A} = (k_{-4A}/k_{+4A})$	9.2(±0.9) μM	Ratio of rate constants
	6.3(±2.1) μM	Ratio of rate constants (global fit)
$K_{4B} = (k_{-4B}/k_{+4B})$	0.01(±0.001)	Ratio of rate constants
$K_{4,overall}$	75(±10) nM	Calculated using Eq. (5)
K_2	77(±25) nM	Detailed balance of Scheme 1
GTP/GMPPNP		
k_{+1}	0.10(±0.01) μM^{-1} s^{-1}	mantGTP binding[10]
k_{-1}	0.00005 s^{-1}	GTP and mantGMPPNP dissociation[11]
K_1	0.5(±0.1) nM	Ratio of rate constants
K_3	8(±2) μM	mantGMPPNP (Fig. 1)
k_{-4}	0.095(±0.017) s^{-1}	mantGMPPNP (Fig. 1)
k_{+4}	3.2(±0.1) μM^{-1} s^{-1}	mantGTP binding[10]
K_4	30(±5) nM	Ratio of rate constants
K_2	133(±48) nM	Detailed balance of Scheme 1

Table 2. Thermodynamic and kinetic coupling of GTPase exchange factors

	Thermodynamic coupling			Kinetic coupling			
GTPase:GEF	K_4 (nM)	K_1 (nM)	K_4/K_1[a]	k_{-4} (s^{-1})	k_{-1} (s^{-1})	k_{-4}/k_{-1}[b]	Reference
Ran:RCC1	3300	0.006	5.5×10^5	21	2.3×10^{-5}	9×10^5	Klebe *et al.*[13]
Ras:Cdc25	500	0.004	1×10^5	1.78	6×10^{-6}	3×10^5	Guo *et al.*[14] and John *et al.*[15]
Rab8:Mss4[c]	100 000	0.1	1×10^6	0.23	7.2×10^{-4}	320	Itzen *et al.*[16]
Sec4:Sec2	4200	0.6	7×10^4	15.3	6.3×10^{-4}	2.4×10^4	Itzen *et al.*[17]
Ypt51p:Vps9p	38	0.3	125	0.012	2×10^{-5}	600	Esters *et al.*[11]
Ypt1p:TRAPP	75	1.2	62.5	0.17	1.2×10^{-4}	1400	This study

[a] Defined as the ratio of GDP affinity in the presence of GEF to nucleotide affinity in the absence of GEF or, equivalently, K_3/K_2 due to the detailed balance of equilibrium constants from Scheme 1.
[b] Defined as the ratio of the rate constant for GDP dissociation in the presence of GEF to rate constant for GDP dissociation in the absence of GEF; also indicative of fold acceleration of nucleotide exchange due to GEF binding.
[c] Rab8:Mss4 is unique in that thermodynamic coupling is much greater than kinetic coupling due entirely to extremely weak nucleotide affinity in the ternary complex (K_4).

4.8 μM for TRAPP binding to Ypt1p–GDP (K_3) (Table 1). The intercept value defines GDP dissociation from Ypt1p and is indistinguishable from the origin, consistent with a rate constant of 0.00012 s^{-1} for GDP dissociation from Ypt1p (k_{-1}),[10] comparable to the value obtained by others under slightly different buffer conditions ($k_{-1}=6\times10^{-5}$ s^{-1}).[11] Thus, TRAPP accelerates GDP dissociation from Ypt1p by more than 3 orders of magnitude from 0.00012 s^{-1} to 0.17 s^{-1} (i.e., $k_{-4}/k_{-1}=\sim1400$; Table 2).

GDP binding to Ypt1p and Ypt1p–TRAPP

GDP binding was measured by rapidly mixing mantGDP with nucleotide-free Ypt1p or Ypt1p–TRAPP complex. Time courses of fluorescence change after mixing Ypt1p with mant-dGDP follow single exponentials with observed rate constants that depend linearly on [mant-dGDP], yielding a second-order association rate constant of 0.1 μM^{-1} s^{-1} for mant-dGDP binding to Ypt1p ($k_{+1,app}$) from the slope of the best-fit line (Fig. 2d,

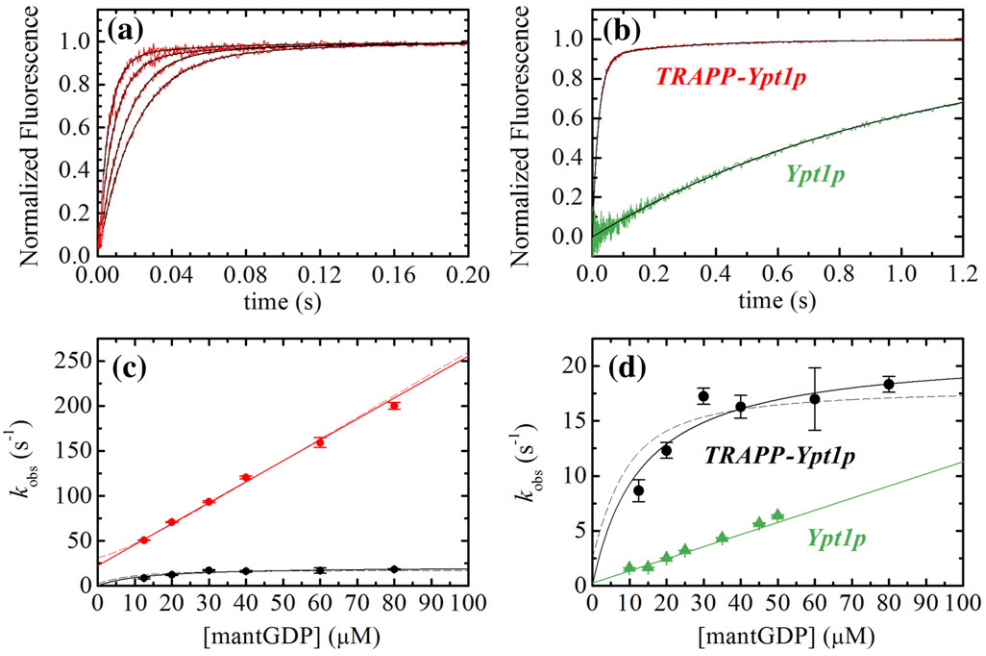


Fig. 2. MantGDP binding Ypt1p and TRAPP–Ypt1p. (a) Time courses of (right to left) 12.5 μM, 20 μM, 40 μM, or 60 μM mantGDP binding to the Ypt1p–TRAPP complex. (b) Time courses of 12.5 μM mantGDP binding to the nucleotide-free Ypt1p (green) or the nucleotide-free TRAPP–Ypt1p (red). The smooth black lines through the data in (a) and (b) represent the best fits to single (Ypt1p) or double (TRAPP–Ypt1p) exponentials. (c) [MantGDP] dependence of the observed rate constant for mantGDP binding to the Ypt1p–TRAPP complex. (d) Concentration dependence of the slow phase for mantGDP binding to the Ypt1p–TRAPP complex. The continuous lines through the data in (c) and (d) represent the best fit to a straight line (Eq. (3)) and hyperbola (Eq. (4)) for fast and slow phases, respectively. The broken lines represent the global fit for all data to the quadratic rate equation (Eq. (2)). MantGDP binding to Ypt1p alone (green triangles), with the best fit of data to a straight line,[10] is shown for comparison.

triangles). We did not observe saturation of the observed rate constant as reported for unlabeled GDP[11] due to the limited range of [mantGDP] examined, so $k_{+1,app}$ describes the overall two-step binding reaction, including the nonspecific collision complex (i.e., $k_{+1,app} = K_0 k_{+1}$, where K_0 is the equilibrium constant for Ypt1p–GDP collision complex formation). The intercept is indistinguishable from the origin, consistent with the slow GDP dissociation rate constant of $k_{-1} = 1 \times 10^{-4}$ s^{-1} measured previously by filter binding and mantGDP dissociation[10] (Table 1).

To determine the effect of TRAPP on GDP association, we measured the kinetics of mantGDP and mant-dGDP binding to the nucleotide-free Ypt1p–TRAPP complex. Time courses of mantGDP and mant-dGDP binding to the complex follow double exponentials, with fast-phase-observed rate constants (k_{fast}) that depend linearly on mantGDP concentration over the range examined (Fig. 2c) and slow-phase-observed rate constants (k_{slow}) that depend hyperbolically on mantGDP concentration (Fig. 2c and d). The biphasic time courses and mantGDP concentration dependence of the fast and slow phases indicate that mantGDP binding to the Ypt1p–TRAPP complex follows a sequential two-step reaction mechanism (Scheme 3) with population of two high-fluorescence TRAPP–Ypt1p–mantGDP states (indicated by * and ′) that exist in a reversible equilibrium.[18,19]:

$$\text{TRAPP} \cdot \text{Ypt1p} + \text{mGDP} \underset{k_{-4A}}{\overset{k_{+4A}}{\rightleftharpoons}} \text{TRAPP} \cdot \text{Ypt1p} \cdot \text{mGDP}^* \underset{k_{-4B}}{\overset{k_{+4B}}{\rightleftharpoons}} \text{TRAPP} \cdot \text{Ypt1p} \cdot \text{mGDP}'$$

Scheme 3. Reaction scheme for sequential two-step nucleotide binding to TRAPP-Ypt1p.

It is likely that a diffusion-limited nonspecific collision complex in rapid equilibrium with free complex and nucleotide[11,20,21] precedes formation of the first high-fluorescence state, but is omitted from Scheme 3 for simplicity.

Global fitting of the [mantGDP] dependence of fast and slow observed rate constants to the general solution of the differential equations defining the two-step binding mechanism depicted in Scheme 3, as given by the following quadratic equation,[22] yields a mantGDP association rate constant (k_{+4A}) of 2.5 μM^{-1} s^{-1}, a dissociation rate constant (k_{-4A}) of 16 s^{-1}, a forward isomerization rate constant (k_{+4B}) of 11 s^{-1}, and a reverse isomerization rate constant (k_{-4B}) approaching 0, consistent with a rate constant of 0.17 s^{-1} for mantGDP dissociation from the Ypt1p–TRAPP complex (i.e., considerably smaller than k_{+4B}; Fig. 1b; Table 1). The isomerization equilibrium constant ($K_{4B} = k_{-4B}/k_{+4B}$) obtained from the ratio of isomerization rate constants is 0.01, indicating that TRAPP–Ypt1p with bound mantGDP essentially populates only the second high-fluorescence state (indicated by ′) at equilibrium. The lack of a detectable fast phase of dissociation from Ypt1p–TRAPP–mant-dGDP (Fig. 1a) is consistent with GDP dissociation exclusively from the TRAPP–Ypt1p–mantGDP′ state (i.e., if the TRAPP–Ypt1p–mantGDP* state were populated at equilibrium, a fast GDP dissociation at ~20 s^{-1} would be observed[18,22]). Independent fitting of the fast and slow phases to linear and hyperbolic equations, which apply when $k_{+4A}[\text{mantGDP}] \gg k_{+4B}$,[18,19]

$$k_{fast} = k_{+4A}[\text{mant–GDP}] + k_{-4A} \quad (3)$$

$$k_{slow} = k_{+4B}\left(\frac{k_{+4A}[\text{mant–GDP}]}{k_{+4A}[\text{mant–GDP}] + k_{-4A}}\right) + k_{-4B} \quad (4)$$

yielded comparable results ($k_{+4A} = 2.4$ μM^{-1} s^{-1}, $k_{-4A} = 22$ s^{-1}, and $k_{+4B} = 21$ s^{-1}; Table 1).

The overall TRAPP–Ypt1p–mantGDP binding affinity (dissociation equilibrium constant $K_{4,overall}$), accounting for the equilibrium population of both high-fluorescence states, can be calculated from:[19]

$$K_{4,overall} = K_{4A}\left(\frac{K_{4B}}{1 + K_{4B}}\right) \quad (5)$$

where the coefficient $K_{4B}/(1 + K_{4B})$ accounts for the contributions of the isomerization equilibrium to the overall affinity. The overall affinity for mantGDP binding to TRAPP–Ypt1p ($K_{4,overall}$) is 75 nM (Table 1), <100-fold weaker than the affinity of mantGDP for Ypt1p in the absence of TRAPP ($K_1 = 1$ nM; Table 1).

Interaction of Ypt1p–TRAPP with GTP and GMPPNP

Since activation of GTPases by GEFs is a process comprising dissociation of bound GDP and binding of GTP, we determined the effects of TRAPP on GTP binding and GMPPNP binding and dissociation from Ypt1p.[10] We previously reported values of 0.1 μM^{-1} s^{-1} and 3.2 μM^{-1} s^{-1} for GTP binding to Ypt1p and TRAPP–Ypt1p, respectively[10] (Table 1). Due to the intrinsic rate of the hydrolysis of GTP by Ypt1p, we measured the dissociation of the slowly hydrolyzing GTP analog mantGMPPNP from Ypt1p as reported above for mantGDP. It has been shown that GMPPNP behaves similarly to GTP in binding to GTPases, including Ypt1p,[11] although GMPPNP conformation may differ in some aspects from GTP conformation (see Henn *et al.*[22] and Yengo *et al.*[23]).

MantGMPPNP dissociates slowly from Ypt1p with a rate constant of 5×10^{-5} s^{-1}.[11] TRAPP accelerates

$$k_{fast,slow} = \frac{(k_{+4A}[\text{GDP}] + k_{-4A} + k_{+4B} + k_{-4B}) \pm \sqrt{(k_{+4A}[\text{GDP}] + k_{-4A} + k_{+4B} + k_{-4B})^2 - 4(k_{-4B}k_{-4A} + k_{-4B}k_{+4A}[\text{GDP}] + k_{+4B}k_{+4A}[\text{GDP}])}}{2} \quad (2)$$

mantGMPPNP exchange from Ypt1p with observed dissociation rate constants that depend hyperbolically on [TRAPP] (Fig. 1b). The best fit of the data to Eq. (1) yields a dissociation rate constant from the ternary complex (k_{-4}) of 0.09 s^{-1}, which represents a ~2000-fold acceleration over the rate of dissociation in the absence of TRAPP, comparable to the ~1400-fold acceleration of GDP dissociation from Ypt1p by TRAPP (Tables 1 and 2). The affinity of TRAPP binding to Ypt1p–GMPPNP (K_3) is 8 μM (Table 1).

Affinity of TRAPP for nucleotide-free Ypt1p

Four equilibrium constants define the interaction of Ypt1p with nucleotide and TRAPP (Scheme 1). Knowledge of the equilibrium constants (Table 1) for nucleotide binding to Ypt1p (K_1 in Scheme 1) and Ypt1p–TRAPP (K_4), and for TRAPP binding to Ypt1p with bound nucleotide (K_3) allows us to calculate the affinity of TRAPP for nucleotide-free Ypt1p (K_4) from the principle of detailed balance. The product of the equilibrium constants of a closed cyclic reaction scheme with no external energy input (e.g., Scheme 1) must be equal to unity. Therefore, $K_2 = K_1K_3/K_4$ when the affinities are expressed as dissociation equilibrium constants. The K_2 value calculated from the experimentally determined equilibrium constants for GDP and GTP/GMPPNP cofactor binding agrees within a factor of 2 (77 nM for GDP parameters and 133 nM for GTP/GMPPNP parameters; Table 1) and indicates that bound nucleotide weakens the affinity of TRAPP for Ypt1p by ~80-fold. Conversely, TRAPP weakens the affinity of Ypt1p for nucleotide by the same amount. The <2-fold discrepancy in K_2 calculated from GDP *versus* GTP/GMPPNP parameters could be attributed, at least in part, to the use of the mantGMPPNP analog to measure K_3 and k_{-4} for GTP.

Mg^{2+} dependence of GDP dissociation from Ypt1p

Numerous guanine and adenine nucleotide binding protein exchange factors, including GEFs for GTPases,[24] actin filaments for myosin V,[19] microtubules for kinesin,[25] and profilin for actin monomers,[26] accelerate nucleotide exchange by disrupting coordination of the nucleotide-associated magnesium cation. Two of these exchange factors (profilin–actin and actin–myosin V) do not accelerate

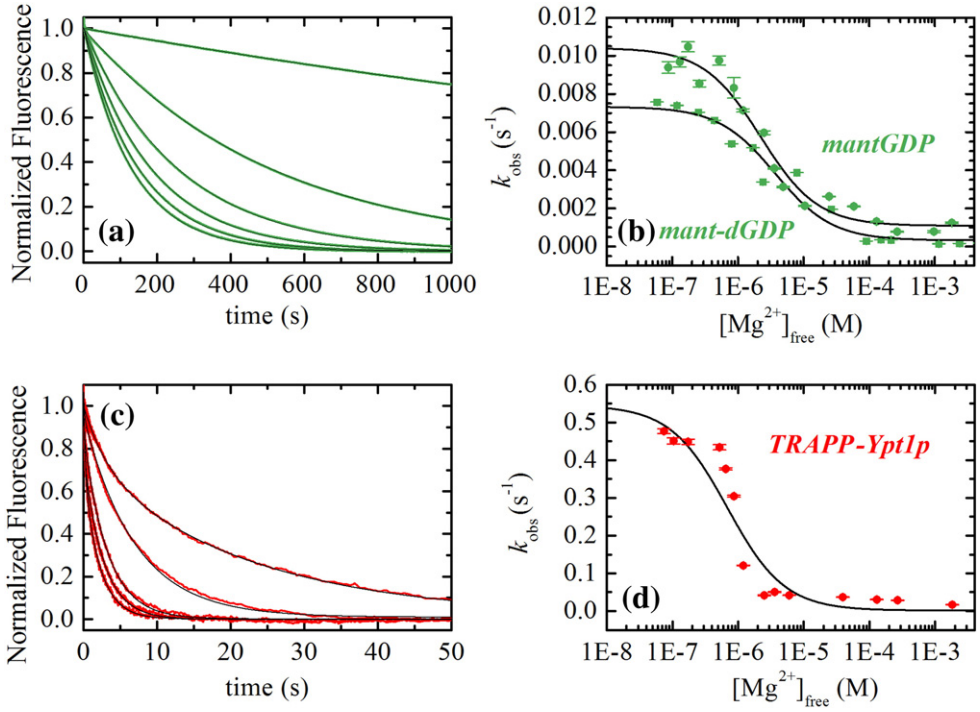


Fig. 3. Mg^{2+} dependence of GDP dissociation from Ypt1p and TRAPP–Ypt1p. (a) Time courses of mant-dGDP dissociation after mixing 250 nM Ypt1p–mantGDP with excess GDP in a buffer containing (left to right) 0.06 μM, 0.44 μM, 0.8 μM, 7.9 μM, 26.6 μM, or 90.3 μM free Mg^{2+} (final). (b) [Mg^{2+}] dependence of the observed rate constants for mant-dGDP (squares) or mantGDP (circles) dissociation from Ypt1p. The smooth black lines through the data (green) represent the best fit to a hyperbola (Eq. (6)) yielding K_{Mg}^{YD} = 3.7 μM, k_{-1}' = 0.0073 s^{-1}, and k_{-1} = 0.00032 s^{-1} for mant-dGDP, and K_{Mg}^{YD} = 2.2 μM, k_{-1}' = 0.0104 s^{-1}, and k_{-1} = 0.0011 s^{-1} for mantGDP. (c) Time courses of mantGDP dissociation after mixing 500 nM Ypt1p–mantGDP with excess GDP in a buffer containing (left to right) 0.87 μM, 2.5 μM, 4.9 μM, 10.5 μM, or 130 μM free Mg^{2+} (final) and 2.5 μM TRAPP. The smooth black lines through the data (red) represent the best fits to double exponentials; the small fast phase shows little [Mg^{2+}] dependence and is observed only with mixed 2′- and 3′-mant isomers. (d) [Mg^{2+}] dependence of mantGDP dissociation from Ypt1p in the presence of 2.5 μM TRAPP. The smooth black lines through the data (red) represent the best fit to a hyperbola (Eq. (7)) yielding $K_{0.5}$ = 1.0 μM, k_∞ = 0.0014 s^{-1}, and k_0 = 0.55 s^{-1} for mantGDP.

nucleotide exchange in the absence of Mg^{2+}. To determine whether nucleotide binding and TRAPP binding are linked through the bound Mg^{2+} and whether TRAPP accelerates nucleotide exchange from Ypt1p by disrupting Mg^{2+} coordination, we measured the Mg^{2+} dependence of mantGDP dissociation from Ypt1p and TRAPP–Ypt1p.

The observed rate constant of mant-dGDP and mantGDP dissociation from Ypt1p (Fig. 3a and b) depends on [Mg^{2+}], dissociating more rapidly at low free [Mg^{2+}]. We assume that the observed effect of Mg^{2+} arises from interaction with the nucleotide, although secondary binding sites on the protein(s) cannot be excluded, and we modeled the data according to Scheme 4:

$$\begin{array}{ccc} \text{Ypt1p} \bullet \text{MgGDP} & \xrightarrow{k_{-1}} & \text{Ypt1p} + \text{MgGDP} \\ \uparrow\downarrow K_{Mg}^{YD} & & \\ \text{Ypt1p} \bullet \text{GDP} & \xrightarrow{k_{-1}'} & \text{Ypt1p} + \text{GDP} \end{array}$$

Scheme 4. Reaction scheme depicting pathways for GDP dissociation from Ypt1p in the presence and absence of Mg^{2+}.

Mg^{2+} binding (K_{Mg}^{YD}) equilibrates more rapidly than GDP dissociates from Ypt1p and is treated as a rapid equilibrium. The best fits of the [Mg^{2+}] dependence of the observed mant-dGDP dissociation rate constant to Eq. (6) (see Appendix):

$$k_{obs} = \frac{(k_{-1} - k_{-1}')[Mg]}{[Mg] + K_{Mg}^{YD}} + k_{-1}' \qquad (6)$$

yields a rate constant of ~0.01 s^{-1} for divalent cation-free mantGDP dissociation (k_{-1}'), ~10-fold more rapid that the Mg-mantGDP dissociation rate constant (k_{-1} ~ 0.001 s^{-1}), and an affinity (K_{Mg}^{YD}) of ~2 μM for Mg^{2+} binding to Ypt1p–mantGDP (Table 3). The k_{-1} value determined from the best fit of the data compares within a factor of 3 to the value measured using radiolabeled nucleotide.[10] Measurements with mant-dGDP yielded parameters that differed by less than a factor of 2 (Table 3).

As with Ypt1p alone, mantGDP dissociation from TRAPP–Ypt1p depends hyperbolically on [Mg^{2+}] and dissociates more rapidly at low free [Mg^{2+}] (Fig. 3c and d). The best fit of the data acquired in the presence of 2.5 μM TRAPP to the following equation (Appendix):

$$k_{obs} = \frac{(k_{\infty} - k_0)[Mg]}{K_{0.5} + [Mg]} + k_0 \qquad (7)$$

yields values of 0.0014 s^{-1} for k_{∞}, 0.55 s^{-1} for k_0, and 1.0 μM for $K_{0.5}$. These observed fitting parameters can be used to extract the fundamental rate and equilibrium binding constants (see Appendix). The observation that the $K_{0.5}$ values (i.e., apparent Mg^{2+} affinity) are similar, within experimental uncertainty, in the presence and in the absence of TRAPP indicates that the Mg^{2+} binding affinity of Ypt1p is not affected by TRAPP (Eq. (A10) of Appendix; Table 3). The dissociation rate constant of divalent cation-free mantGDP from TRAPP–Ypt1p (k_{-4}'; calculated using Eq. (A11)) is ~1.6 s^{-1}, ~10-fold more rapid than the dissociation of Mg–mantGDP (k_{-4} ~ 0.17 s^{-1}; Table 1). A 10-fold acceleration of GDP release from Ypt1p by ethylenediaminetetraacetic acid (EDTA) is also observed in the absence of TRAPP (Table 3), consistent with Mg^{2+} binding to Ypt1p being independent of TRAPP interactions.

Table 3. Rate and equilibrium constants for Mg^{2+}-dependent GDP exchange

$$\begin{array}{ccccc} \text{Ypt1p} + \text{MgGDP} & \overset{K_1}{\rightleftharpoons} & \text{Ypt1p} \bullet \text{Mg} \bullet \text{GDP} & \overset{K_3}{\rightleftharpoons} & \text{TRAPP} \bullet \text{Ypt1p} \bullet \text{Mg} \bullet \text{GDP} & \overset{K_4}{\rightleftharpoons} & \text{TRAPP} \bullet \text{Ypt1p} + \text{MgGDP} \\ \downarrow\uparrow K_{Mg}^{D} & & \downarrow\uparrow K_{Mg}^{YD} & & \downarrow\uparrow K_{Mg}^{TYD} & & \downarrow\uparrow K_{Mg}^{D} \\ \text{Ypt1p} + \text{GDP} + \text{Mg} & \overset{K_1'}{\rightleftharpoons} & \text{Ypt1p} \bullet \text{GDP} & \overset{K_3'}{\rightleftharpoons} & \text{TRAPP} \bullet \text{Ypt1p} \bullet \text{GDP} & \overset{K_4'}{\rightleftharpoons} & \text{TRAPP} \bullet \text{Ypt1p} + \text{GDP} \end{array}$$

Parameter	Value	Source
K_1	1.2(±0.2) nM	Ratio of rate constants (Table 1)
K_3	4.8(±1.2) μM	mantGDP/mant-dGDP (Fig. 1; Table 1)
K_4	75(±10) nM	Calculated using Eq. (5) (Table 1)
K_{Mg}^{D}	842(±32) μM	Isothermal titration calorimetry
K_{Mg}^{YD}	2.2(±0.5) μM	mantGDP (Fig. 3b)
	3.7(±1.1) μM	mant-dGDP (Fig. 3b)
K_{Mg}^{TYD}	1.0(±0.3) μM	mantGDP (Fig. 3d)
K_1'	460(±130) nM	Detailed balance ($K_1K_{Mg}^{D}/K_{Mg}^{YD}$)
k_{-1}'	0.0073(±0.0004) s^{-1}	mant-dGDP (Fig. 3b)
	0.0104(±0.0004) s^{-1}	mantGDP (Fig. 3b)
k_{+1}'	0.02(±0.006) μM^{-1} s^{-1}	Calculated from ratio
K_3'	~5 μM	Detailed balance ($K_3K_{Mg}^{YD}/K_{Mg}^{TYD}$)
K_4'	~30 μM	Detailed balance ($K_4K_{Mg}^{D}/K_{Mg}^{TYD}$)
k_{-4}'	1.6(±0.3) s^{-1}	Eq. (A11) (Fig. 3d)
k_{+4}'	0.05 μM^{-1} s^{-1}	Calculated from ratio

Equilibrium constants K_1–K_4 are the same as in Scheme 1, while K_1'–K_4' represent corresponding equilibria in the absence of Mg^{2+}. The equilibrium constants representing Mg^{2+} binding are indicated with subscript Mg and superscripts D, YD, and TYD representing binding to GDP, Ypt1p–GDP, and TRAPP–Ypt1p–GDP, respectively.

Discussion

Mechanism of nucleotide exchange catalysis by TRAPP differs from those of other characterized GEFs

GEFs activate GTPases by accelerating the dissociation of bound nucleotide up to several orders of magnitude. For the large majority of GTPase–GEF systems examined, GEF binding significantly weakens the nucleotide binding affinity of the associated GTPase, and a general exchange strategy has been proposed in which nucleotide exchange is catalyzed through an allosteric mechanism thermodynamically driven by a GEF-linked reduction in nucleotide binding affinity and reciprocal nucleotide-dependent reduction in GEF affinity.[2,14] In most cases, thermodynamic linkage is similar whether GDP or GTP is bound, and exchange of GDP for GTP is favored by the higher concentration and chemical potential of cytosolic GTP. Nucleotide binding to the GTPase–GEF complex is weak because GEF alters the configuration of the nucleotide-binding pocket—typically in the conformations of switch I or switch II, the regions of GTPase nucleotide-binding pocket that differ in active and inactive conformations.[27] In many instances, as revealed by structural studies of GEF–GTPase complexes,[28–30] this is accomplished by insertion of a structural element from the GEF (a "wedge") into the nucleotide-binding pocket of the GTPase to either directly inhibit the binding of nucleotide or indirectly inhibit binding by blocking the Mg^{2+} required for coordination of its negatively charged phosphates.

The crystal structure of nucleotide-free Ypt1p with bound TRAPP[10] shows that, like all known GEFs, TRAPP reorganizes the nucleotide-binding pocket of Ypt1p. Both switch I and switch II have altered conformations as compared with the nucleotide-bound state (in the absence of TRAPP); as a result of the switch I rearrangement, the nucleotide-binding pocket is opened to the solvent. The C-terminus of one of the TRAPP subunits, Bet3p, is inserted into the Ypt1p nucleotide-binding site,[10] where it occupies a position that is partially occupied by switch I in nucleotide-bound forms of Ypt1p. The Bet3p C-terminus is unusual as a wedge, however, in that it is not a rigid structural element and, in the absence of Ypt1p, it is unstructured (see, e.g., Protein Data Bank entries 2J3W and 2J3T).[9] Although the Bet3p C-terminus is essential for activity,[10] it is likely that it assumes the position observed in the structure only after the initial encounter of Ypt1p with TRAPP and does not function as a typical wedge to sterically displace bound nucleotide. It is also worth noting that, with one exception (switch I residue Tyr33, which forms an aromatic–aromatic interaction with the guanosine base of bound nucleotide), few of the GTPase residues that interact with nucleotide directly are perturbed in the Ypt1p–TRAPP complex.[10] We had, therefore, previously hypothesized that TRAPP facilitates nucleotide exchange not by weakening the nucleotide affinity of Ypt1p but by opening the nucleotide-binding pocket and by making it easier for nucleotides to bind and dissociate.[10] The biochemical solution studies completed in this study support this hypothesis and favor a mechanism in which TRAPP GEF activity occurs with weak thermodynamic linkage through a Mg^{2+}-independent pathway.

The TRAPP–Ypt1p thermodynamic linkage is weak because TRAPP accelerates both dissociation and association of nucleotide, (a) allowing Ypt1p to equilibrate more rapidly with free GTP in solution (kinetic basis of GEF activity) but also (b) yielding small net changes in overall nucleotide binding affinity (thermodynamic basis of GEF activity). Such a considerable acceleration in nucleotide binding to GTPases when bound to GEFs is uncommon and suggests a unique pathway for TRAPP modulating the Ypt1p nucleotide-binding site.

Theoretical values for the maximum association rate constant for a diffusion-limited reaction can be approximated from the Smoluchowski equation (Eq. (8)):[31]

$$k_{\text{collision}} = 4\pi(D_A + D_B)(r_A + r_B)N_0 10^{-3} \qquad (8)$$

where $k_{\text{collision}}$ is the collision rate constant, D_A and D_B are the translational diffusion coefficients (in $cm^2\ s^{-1}$) for the two species, r_A and r_B are the interaction radii (in cm), and N_0 is Avogadro's number (the factor 10^{-3} is required for conversion into units of M^{-1}). The diffusion coefficient and radius for GDP can be approximated by those values calculated for Mg^{2+}-ATP[32,33] as $r_{GDP} = 4\times10^{-8}$ cm, with corresponding $D = 6.13\times10^{-6}\ cm^2\ s^{-1}$ at 25 °C. The translational diffusion coefficient for Ypt1p estimated from the Stokes–Einstein relation using the radius approximated from the crystal structure[10] is $1.2\times10^{-6}\ cm^2\ s^{-1}$, and the radius of the nucleotide-binding site is estimated to be approximately equal in size to GDP. These values yield a value of $\sim4.5\times10^9\ M^{-1}\ s^{-1}$ for $k_{\text{collision}}$, which is more than 4 orders of magnitude greater than the rate constant for GDP binding to Ypt1p. This means that ~1 in 50,000 random collisions between nucleotide and the Ypt1p nucleotide-binding site results in productive binding.

Binding constants this far below the diffusion limit often arise from multistep binding and/or an inaccessible ligand-binding site (see Robblee *et al.*,[20,21] De La Cruz and Pollard,[34,35] and Cao *et al.*[36]). The latter could result if nucleotide-free Ypt1p were partially denatured and adopted a conformation incapable of readily binding nucleotide. Multistep nucleotide binding to Ypt1p has been observed; GDP and GTP binding follow a two-step mechanism with formation of a low-affinity nonspecific collision complex ($K_{\text{coll}} = \sim300\ \mu M$) that isomerizes slowly ($k_{\text{isom}} \sim 40\ s^{-1}$, where $k_{\text{isom}} =$

$k_{+isom}+k_{-isom}$ and $k_{-isom}\approx k_{-1}\approx 10^{-4}$ s^{-1}) to a conformation that binds nucleotide strongly,[11] yielding an overall association rate constant (k_{+isom}/K_{coll}) of ~ 0.1 μM^{-1} s^{-1}, as reported in this study. The value of K_{coll} is in the same range as other proteins that bind nucleotide rapidly (see, e.g., Robblee *et al.*[20] and De La Cruz *et al.*[37]) and is an order of magnitude tighter than proteins that equilibrate between states with accessible and inaccessible nucleotide-binding site conformations (see, e.g., Robblee *et al.*[20,21] and De La Cruz *et al.*[38]). In contrast, an isomerization rate constant of 40 s^{-1} is very slow when compared to other nucleotide-binding proteins (see, e.g., Robblee *et al.*[21] and De La Cruz *et al.*[37]). These characteristics suggest that an inactive conformation of nucleotide-free Ypt1p does not account for the slow Ypt1p–nucleotide association kinetics. Rather, they indicate that slow nucleotide binding to Ypt1p arises because of a slow isomerization rate constant.

The rate constant for GDP binding to Ypt1p is >20-fold more rapid in the presence of TRAPP, increasing the number of productive collisions to ~1 in every 1000 and the overall association rate constant to ~ 2 μM^{-1} s^{-1}, comparable to values observed for other nucleotide-binding proteins.[18,21,22,33,39] Acceleration of nucleotide binding would arise if TRAPP made K_{coll} tighter and/or accelerated k_{isom}. The observation that the rate of nucleotide binding to TRAPP–Ypt1p is considerably faster than 40 s^{-1} at subsaturating nucleotide concentrations (Fig. 2c) indicates that TRAPP increases k_{isom} by at least an order of magnitude. It is possible that K_{coll} could also be tighter when TRAPP is bound, thereby also contributing to faster nucleotide binding. However, K_{coll} for nucleotide binding to TRAPP–Ypt1p is >100 μM, as indicated by the lack of a hyperbolic dependence of k_{obs} on nucleotide concentrations of up to 80 μM (Fig. 2c). These observations indicate that TRAPP promotes nucleotide binding to Ypt1p by accelerating weak to strong nucleotide binding isomerization (k_{+isom}) from ~40 s^{-1} to >200 s^{-1}. Because TRAPP also accelerates the reverse isomerization rate constant (k_{-isom}), which precedes and limits nucleotide dissociation, it can be viewed as effectively lowering the transition-state energy barrier between weak and strong nucleotide-binding states.

The Mg^{2+} dependence of GDP dissociation (Fig. 3) also supports the interpretation that catalysis of nucleotide exchange by TRAPP differs from the mechanism of other characterized GEFs, including Tiam1 (Rho GEF),[40] Trio (Rho GEF),[41] Sos (Ras GEF),[29] Rabex-5 (Rab GEF),[42] Sec2 (Rab GEF),[43] and Sec7 (Arf GEF).[30] Binding of GEFs typically results in structural rearrangements in the nucleotide-binding pocket of the associated GTPase that competes with bound Mg^{2+}, either through the use of a GEF "glutamate finger"[30] or through the use of residues from the GTPase itself that are shifted into the Mg^{2+}-binding site,[29,40,43] thereby weakening the overall Mg^{2+} and, consequently, GDP binding affinities.[41] The Mg^{2+} affinity for Ypt1p–mantGDP is unaffected by TRAPP (Table 3), indicating that the TRAPP and nucleotide-binding sites do not communicate allosterically by weakening the Mg^{2+} affinity, as observed for other GEFs[24,27] and adenine nucleotide exchange factors.[19,25,26] In fact, TRAPP is better than EDTA at dissociating GDP from Ypt1p, indicating that TRAPP activation is not due to prevention of Mg^{2+} rebinding at the nucleotide-binding site. Contributions to acceleration of nucleotide dissociation via a Mg^{2+}-independent pathway have been reported for H-Ras nucleotide exchange by Cdc25[44] and for Rac1 nucleotide exchange by Trio.[41] Here we provide evidence that a GEF can function without any perturbation of Mg^{2+} affinity. Since disruption of Mg^{2+} coordination is not the source of allostery and acceleration of nucleotide exchange, TRAPP GEF activity must be mediated through an alternative mechanism. Although perturbation of bound Mg^{2+} coordination may occur, it does not account for the acceleration of GDP dissociation, and additional factors such as reorganization of switch I must also contribute to acceleration of nucleotide binding and dissociation.

Kinetic *versus* thermodynamic control of nucleotide exchange

Catalysis of nucleotide exchange from Ypt1p by TRAPP occurs without a large overall weakening of nucleotide binding affinity (Tables 1 and 2). While most GEFs significantly weaken GDP affinity by >10,000-fold from less than nanomolar to micromolar affinities (Table 2, columns 2 and 3), TRAPP weakens the affinity by only ~100-fold. However, GDP dissociation from Ypt1p is accelerated by >1000-fold by TRAPP (Table 1), making TRAPP an efficient nucleotide exchange factor. Therefore, whereas thermodynamics drives nucleotide exchange for most GEFs by weakening the affinity of the GTPase for nucleotides, a strong energetic coupling of linked nucleotide- and GEF-binding sites does not drive TRAPP GEF activity. Thus, TRAPP GEF activity can be viewed as under kinetic, rather than thermodynamic, control. The nucleotide exchange factor for actin monomers, profilin, also functions using similar principles.[39]

Degree of thermodynamic coupling and biological consequences

Nucleotide exchange can be considered from the viewpoint of energetic coupling between nucleotide and exchange factor binding to the GTPase (Scheme 1) such that GEF binding weakens affinity for nucleotide and, consequently, nucleotide weakens affinity for GEF.[2] In other words, GEF and nucleotide binding are linked, and acceleration of nucleotide exchange is a consequence of strong coupling between nucleotide and GEF binding. The degree of thermodynamic coupling is given by the ratio of K_4/K_1 or, equivalently, K_3/K_2 (Scheme 1). A high thermodynamic coupling ratio (Table 2) indicates

strong coupling and is a measure of how much binding of one ligand weakens the affinity of the other.

The affinity of mantGDP for Ypt1p is reduced by ~100-fold with TRAPP binding (thermodynamic coupling ratio ~100). The corresponding coupling ratio for most other characterized GEFs is $\sim 10^4$ to 10^6 (Table 2). In many of these cases, the weaker nucleotide affinity largely scales with the acceleration in exchange rate (k_{-4}). That is, there is a correlation between the degree of thermodynamic coupling indicated by K_4/K_1 and the degree of "kinetic coupling" or "kinetic effectiveness"[2] (i.e., acceleration of nucleotide dissociation) indicated by k_{-4}/k_{-1}. Thus, for these systems, acceleration of nucleotide exchange is a consequence of strong thermodynamic and kinetic coupling between GEF and nucleotide binding. This is not the case for TRAPP, where kinetic coupling is considerably stronger than thermodynamic coupling, thereby allowing TRAPP to function as an effective exchange factor due to kinetic destabilization of bound nucleotide. Such a mechanism for an effective GEF with weak thermodynamic coupling was hypothesized from a theoretical perspective, although no example had been documented.[2]

Another notable exception is the Rab Ypt51p and its associated GEF Vps9. In this system, nucleotide affinity is weakened by ~100- to 1000-fold.[11] There is a corresponding ~600-fold acceleration of nucleotide dissociation, which accounts for the weakened affinity. In this case also, binding of Vps9 does not reduce nucleotide affinity as much as with other Ras-like GTPases (i.e., thermodynamic coupling is low). This situation differs from the Ypt1p–TRAPP system, however, in that the kinetic and thermodynamic coupling ratios are similar. It is interesting to note that both of these systems with weak thermodynamic coupling are Rabs involved in membrane trafficking pathways, raising the possibility that a relationship between the mechanism of nucleotide exchange and vesicle transport has evolved (discussed below). However, another Rab Sec4p, which functions in exocytosis, and its GEF, Sec2p, have similar thermodynamic and kinetic coupling ratios,[17] in keeping with parameters observed for other Ras subfamilies of GTPases (Table 2).

Most characterized GTPases have high thermodynamic coupling ratios and, in consequence, exist as one of the two binary complexes (with bound nucleotide or bound to GEF in the nucleotide-free state), with the ternary complex comprising a negligible fraction of the total GTPase pool. The direct consequence of weak coupling between nucleotide binding and TRAPP binding to Ypt1p is that the ternary (TRAPP–Ypt1p–nucleotide) complex is stable and can be populated to a significant extent under physiological conditions. In support of this prediction, TRAPP is capable of binding both GDP-bound and GTP-bound forms of Ypt1p in yeast cell lysates, as determined from pull-down assays.[10] As a result of the weak coupling, TRAPP can activate Ypt1p by accelerating GDP dissociation and GTP binding without destabilization of the complex. DSS4, another protein that accelerates nucleotide dissociation from Ypt1p, also forms a stable complex with Ypt1p; however, in this case, the nucleotide-free DSS4–Ypt1p is significantly favored.[11] In addition, DSS4 is a far less efficient exchange factor than TRAPP—so weak that it is generally not considered to be a *bona fide* GEF.

Weak coupling between nucleotide binding and exchange factor binding is demonstrated in other systems in which population of the ternary complex is important for biological function. Most notably, the degree of coupling between ADP and actin binding correlates with the biological function of myosin motors.[45,46] Myosin motors with weak thermodynamic coupling populate the ternary actomyosin–ADP complex and operate as tension sensors and processive transporters. Myosin motors with strong thermodynamic coupling do not populate the ternary complex and operate as "fast movers" that generate rapid contractions and transport.

In a similar manner, formation of the ternary Ypt1p–TRAPP–nucleotide complex could potentially reflect an adaptation for the biological activity of TRAPP. GEF activity of TRAPP-I and activation of Ypt1p are critical for endoplasmic-reticulum-derived COPII transport vesicle fusion with the Golgi apparatus. Upon activation of Ypt1p, the weak thermodynamic coupling ensures that a significant fraction of the activated Ypt1p–GTP remains bound to the TRAPP complex. The stable ternary complex of TRAPP with GTP-bound Ypt1p would permit effector proteins that are substrates for Ypt1p to be recruited within the vicinity of the site of vesicle fusion, thereby allowing all components required for fusion to be colocalized around the TRAPP tethering complex; if the ternary complex affinity were very weak, Ypt1p could potentially recruit components of membrane fusion at sites where TRAPP is not localized. In this manner, TRAPP GEF activity is kinetically tuned to be an effective GEF activator of Ypt1p and thermodynamically adapted to localize activated Ypt1p at sites of membrane fusion, in accordance with TRAPP functioning as a tethering complex with GEF activity.

Clearly, this behavior relies on the ability to form a ternary TRAPP–Ypt1p–nucleotide complex. Although the measured K_d of TRAPP to GTP-bound Ypt1p is ~5 μM while estimates of the cellular concentration of TRAPP are ~100 nM (based on TRAPP comprising 0.01% of the total cell protein, ~6 pg of proteins per haploid cell, and assuming a spherical yeast cell with a 5-μm diameter; S.F.-N., unpublished observation), local effective concentrations of TRAPP can be considerably higher due to the association of these proteins with membranes, as suggested for other Rabs with their GEFs.[17] It is also possible that

subunits of TRAPP-I and TRAPP-II that are absent in the TRAPP subcomplex used in this study may further increase the affinity for nucleotide-bound Ypt1p, as could crowded cellular conditions.[47]

Materials and Methods

Reagents

All reagents were of the highest purity grade commercially available. Mixed 2′- and 3′-mant nucleotides were purchased from Invitrogen, and single mant-dGDP and 2′-deoxy mantGTP isomers were purchased from Jena Biosciences. One molar equivalent of $MgCl_2$ was added to the nucleotide immediately before use.

Protein expression and purification

TRAPP proteins and Ypt1p were expressed and purified as described.[10] TRAPP subcomplexes comprised Bet3p, Bet5p, Trs23p, Trs31p, and Trs20p (without Trs33p), which contained all essential TRAPP subunits and were indistinguishable from intact TRAPP-I in guanine nucleotide exchange activity.[8,9] Briefly, for overexpression of TRAPP subcomplexes, three Duet plasmids harboring genes for *BET3*, *BET5*, *TRS23*, *TRS31*, and *TRS20* were cotransformed into *Escherichia coli* BL21(DE3) cells by electroporation, and protein expression was induced with 0.5 mM IPTG. Cells were harvested 18 h after induction. TRAPP subcomplex was purified by Ni-NTA chromatography (Qiagen). Gel filtration over a Superdex-200 column (GE Healthcare) removed the Bet3p/Trs31p heterodimer.

An N-terminal His-tagged Ypt1p construct truncated at amino acid 180 (His_6-Ypt1p 1–180) was overexpressed in *E. coli* BL21(DE3) cells at 25 °C and purified using Ni-NTA resin (Qiagen). Nucleotide-free Ypt1p was prepared with EDTA[13,48] or with alkaline phosphatase treatment for 12 h at 16 °C[49] to remove bound GDP. Essentially identical results were obtained with both preparation methods. Nucleotide-free Ypt1p was used immediately after preparation, as it became inactive when stored overnight on ice. Ypt1p with bound mantGDP was prepared by mixing labeled nucleotide and 5 mM Mg^{2+} (free) with nucleotide-free Ypt1p. Excess mant–nucleotide was removed by gel filtration over a Zeba desalt spin column (Pierce).

Nucleotide binding kinetics

Mant–nucleotide binding to Ypt1p was measured from fluorescence enhancement associated with Förster resonance energy transfer from Ypt1p tryptophan residues ($\lambda_{ex} = 280$ nm) to bound fluorescent mant–nucleotide.[10,11,50] Kinetic measurements were made using an Applied Photophysics SX 18MV-R stopped-flow apparatus thermostatted at 25(±0.1) °C. Fluorescence was monitored at 90° through a 400-nm long-pass colored glass filter. The final buffer conditions were 50 mM Tris–HCl (pH 8.0), 100 mM NaCl, 5 mM $MgCl_2$, and 1 mM DTT. Multiple (two to three) time courses were averaged and fitted to a sum of exponentials by nonlinear least-squares regression. Uncertainties are reported as standard errors in the fits, unless otherwise stated. The concentrations stated are final after mixing.

Association kinetics were measured by mixing 250 nM nucleotide-free Ypt1p in the presence or in the absence of 5 μM TRAPP complex under pseudo-first-order conditions with [nucleotide] ≫ [Ypt1p] or [Ypt1p–TRAPP]. GDP exchange from Ypt1p is limited by dissociation of bound GDP and was measured by mixing equilibrated samples of Ypt1p–mantGDP with excess (300 μM–2 mM) unlabeled GDP and the indicated [TRAPP].

The Mg^{2+} dependence of nucleotide exchange was measured by mixing Ypt1p–mantGDP (0.5 μM) with varying concentrations of EDTA and excess (300 μM–2 mM) unlabelled GDP. The final free [Mg^{2+}] was calculated by the Web-based MaxCHELATOR program.

Kinetic simulations

Simulated time courses of TRAPP-accelerated nucleotide exchange (Fig. 1), mantGDP binding to Ypt1p and TRAPP–Ypt1p (Fig. 2), and the Mg^{2+} dependence of GDP dissociation from Ypt1p and TRAPP–Ypt1p (Fig. 3) using the experimental binding parameters (Tables 1 and 3) and the corresponding reaction schemes performed with KinTek Global Explorer confirm that the rate and equilibrium constants accurately account for the experimental data (data not shown). KinTek Global Explorer is based on the kinetic simulation and fitting programs KINSIM and FITSIM developed by Barshop *et al.*[51]

Isothermal titration calorimetry

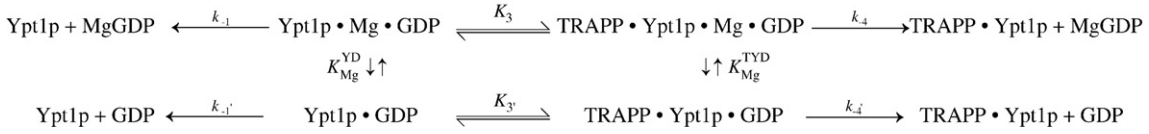
An affinity of 842(±32) μM for Mg^{2+} binding to GDP was measured at 25(±0.1) °C in 50 mM Tris–HCl (pH 8.0), 100 mM NaCl, and 1 mM DTT buffer with a MicroCal (Northampton, MA) MCS isothermal titration calorimeter. Data analysis was performed with Origin software accompanying the instrument.

Acknowledgements

This work was supported by grants from the Hellman Family to E.M.D.L.C. and from the Mathers Foundation and the National Institutes of Health (GM080616) to K.M.R. S.F.-N. is an Investigator of the Howard Hughes Medical Institute, and S.M. is a postdoctoral associate of the Howard Hughes Medical Institute. E.M.D.L.C. is an American Heart Association Established Investigator (0940075 N) and a National Science Foundation CAREER Award recipient (MCB-0546353). E.M.D.L.C. acknowledges additional support from the National Institutes of Health under award GM071688. H.F.C. was supported by National Institutes of Health predoctoral fellowship F31 DC009143-01 and, in part, by grants from the American Heart Association (0655849T) and Yale Institute for Nanoscience and Quantum Engineering to E.M.D.L.C. We thank anonymous referees for insightful comments.

Appendix

The $[Mg^{2+}]$ dependence of irreversible GDP dissociation (exchange) from Ypt1p was analyzed according to Scheme 5, which was adapted from the scheme in Table 3.



Scheme 5. GDP dissociation from Ypt1p in the presence and absence of TRAPP and Mg^{2+}.

Since the dissociation of GDP from any of these four starting complexes of Ypt1p–GDP with Mg^{2+} and/or TRAPP (k_{-1}, k_{-1}', k_{-4}, and k_{-4}') is at least an order of magnitude slower than Mg^{2+} or TRAPP binding and dissociation, equilibrium among these complexes is maintained throughout the course of the experiment (i.e., K_{Mg}^{TYD}, K_3, and K_3' can be treated as rapid equilibria). Under our experimental conditions, free $[Mg^{2+}]$ is constant and can be calculated based on total $[MgCl_2]$, [GDP], and [EDTA] according to the respective equilibrium constants for Mg^{2+} binding.

The observed rate constant of GDP dissociation in the presence of TRAPP represents the weighted average of dissociation from all four nucleotide-bound states and is given by the following differential equation:

$$\frac{d}{dt}\left(\left[\text{Ypt1p} \bullet \text{Mg} \bullet \text{D}\right] + \left[\text{Ypt1p} \bullet \text{D}\right] + \left[\text{TRAPP} \bullet \text{Ypt1p} \bullet \text{Mg} \bullet \text{D}\right] + \left[\text{TRAPP} \bullet \text{Ypt1p} \bullet \text{D}\right]\right) = - k_{-1}\left[\text{Ypt1p} \bullet \text{Mg} \bullet \text{D}\right] - k_{-1}'\left[\text{Ypt1p} \bullet \text{D}\right] - k_{-4}\left[\text{TRAPP} \bullet \text{Ypt1p} \bullet \text{Mg} \bullet \text{D}\right] - k_{-4}'\left[\text{TRAPP} \bullet \text{Ypt1p} \bullet \text{D}\right] \tag{A1}$$

which can be rewritten in terms of any of the four starting complexes of Ypt1p–GDP (plus [TRAPP] and $[Mg^{2+}]_{free}$) and three of the four equilibrium equations in Scheme 5:

$$K_{Mg}^{YD} = \frac{\left[\text{Ypt1p} \bullet \text{GDP}\right]\left[\text{Mg}\right]}{\left[\text{Ypt1p} \bullet \text{Mg} \bullet \text{GDP}\right]} \tag{A2}$$

$$K_3 = \frac{\left[\text{Ypt1p} \bullet \text{Mg} \bullet \text{GDP}\right]\left[\text{TRAPP}\right]}{\left[\text{TRAPP} \bullet \text{Ypt1p} \bullet \text{Mg} \bullet \text{GDP}\right]} \tag{A3}$$

$$K_{Mg}^{TYD} = \frac{\left[\text{TRAPP} \bullet \text{Ypt1p} \bullet \text{GDP}\right]\left[\text{Mg}\right]}{\left[\text{TRAPP} \bullet \text{Ypt1p} \bullet \text{Mg} \bullet \text{GDP}\right]} \tag{A4}$$

$$K_3' = \frac{\left[\text{Ypt1p} \bullet \text{GDP}\right]\left[\text{TRAPP}\right]}{\left[\text{TRAPP} \bullet \text{Ypt1p} \bullet \text{GDP}\right]} \tag{A5}$$

where all Ks represent overall dissociation equilibrium constants.

Rewriting Eq. (A1) in terms of [Ypt1p–Mg–GDP], the biochemical state populated at the start of the experiment (i.e., at $t = 0$) yields:

$$\frac{d}{dt}\left[\text{Ypt1p} \bullet \text{Mg} \bullet \text{GDP}\right] = -\left(\frac{k_{-1}\left(K_3\left[\text{Mg}\right]\right) + k_{-1}'\left(K_{Mg}^{YD}K_3\right) + k_{-4}\left(\left[\text{Mg}\right]\left[\text{TRAPP}\right]\right) + k_{-4}'\left(K_{Mg}^{TYD}\left[\text{TRAPP}\right]\right)}{K_3\left[\text{Mg}\right] + K_{Mg}^{YD}K_3 + \left[\text{Mg}\right]\left[\text{TRAPP}\right] + K_{Mg}^{TYD}\left[\text{TRAPP}\right]}\right)\left[\text{Ypt1p} \bullet \text{Mg} \bullet \text{GDP}\right] \tag{A6}$$

assuming $[Mg^{2+}]_{free}$ and $[TRAPP]_{free}$ are constant with respect to time, which they are under our conditions with [TRAPP] ≫ [Ypt1p]. The solution to the differential equation Eq. (A6) is a single exponential with an observed relaxation rate constant k_{obs} given by the term in parentheses on the right-hand side of Eq. (A6).

In the absence of TRAPP (Fig. 3a), GDP dissociation occurs through k_{-1} and k_{-1}', and k_{obs} of nucleotide exchange depends on $[Mg^{2+}]$ according to:

$$k_{obs} = \frac{k_{-1}\left(K_3\left[\text{Mg}\right]\right) + k_{-1}'\left(K_{Mg}^{YD}K_3\right)}{K_3\left[\text{Mg}\right] + K_{Mg}^{YD}K_3} \tag{A7}$$

which simplifies to:

$$k_{obs} = \frac{k_{-1}([Mg]) + k_{-1}'\left(K_{Mg}^{YD}\right)}{[Mg] + K_{Mg}^{YD}} = \frac{(k_{-1} - k_{-1}')[Mg]}{[Mg] + K_{Mg}^{YD}} + k_{-1}' \quad \text{(A8)}$$

predicting a hyperbolic dependence of k_{obs} on $[Mg^{2+}]$ (Fig. 3b) with an intercept value (k_0; extrapolation to $[Mg^{2+}]=0$) of k_{-1}', a saturating value (k_∞; achieved at $[Mg^{2+}]\rightarrow\infty$) of k_{-1}, and $[Mg^{2+}]$ at a half-maximal saturation ($K_{0.5}$) of K_{Mg}^{YD}.

We measured the $[Mg^{2+}]$ dependence of nucleotide exchange from Ypt1p at a constant nonsaturating [TRAPP] (Fig. 3c and d). Under these conditions, the value of k_{obs} depends hyperbolically on $[Mg^{2+}]$ according to:

$$k_{obs} = \frac{(k_\infty - k_0)[Mg]}{K_{0.5} + [Mg]} + k_0 \quad \text{(A9)}$$

with the following parameters:

$$K_{0.5} = \frac{K_{Mg}^{YD}K_3 + K_{Mg}^{TYD}[TRAPP]}{K_3 + [TRAPP]} = \frac{\left(K_{Mg}^{TYD} - K_{Mg}^{YD}\right)[TRAPP]}{K_3 + [TRAPP]} + K_{Mg}^{YD} \quad \text{(A10)}$$

$$k_0 = \frac{k_{-1}'\left(K_{Mg}^{YD}K_3\right) + k_{-4}'\left(K_{Mg}^{TYD}[TRAPP]\right)}{K_{Mg}^{YD}K_3 + K_{Mg}^{TYD}[TRAPP]} = \frac{(k_{-4}' - k_{-1}')[TRAPP]}{[TRAPP] + \left(\frac{K_{Mg}^{YD}K_3}{K_{Mg}^{TYD}}\right)} + k_{-1}' \quad \text{(A11)}$$

$$k_\infty = \frac{k_{-1}(K_3) + k_{-4}[TRAPP]}{K_3 + [TRAPP]} = \frac{(k_{-4} - k_{-1})[TRAPP]}{K_3 + [TRAPP]} + k_{-1} \quad \text{(A12)}$$

The term k_0 (Eq. (A11)) represents the [TRAPP] dependence of the observed GDP dissociation rate constant in the absence of Mg^{2+} and in the presence of TRAPP (Fig. 3c and d), predicting a hyperbolic dependence on [TRAPP] with an intercept value (i.e., $[TRAPP]=0$) of k_{-1}', a saturating value (i.e., $[TRAPP]\rightarrow\infty$) of k_{-4}', and a $K_{0.5}$ value of $\frac{K_{Mg}^{YD}K_3}{K_{Mg}^{TYD}} = K_3$ (due to detailed balance). k_∞ represents the dependence of the observed rate constant for GDP dissociation in the presence of saturating Mg^{2+} and in the presence of TRAPP (Fig. 1), yielding a hyperbolic [TRAPP] dependence of k_{obs} equivalent to that given in Eq. (1) in the text. Therefore, the intrinsic rate and equilibrium constants K_{Mg}^{TYD} and k_{-4}' can be determined using Eqs. (A10)–(A12) and the experimentally determined values of K_{Mg}^{YD} (Fig. 3a and b), k_{-1}' (Fig. 3a and b), and K_3 (Fig. 1).

References

1. Bourne, H. R., Sanders, D. A. & McCormick, F. (1990). The GTPase superfamily: a conserved switch for diverse cell functions. *Nature*, **348**, 125–132.
2. Goody, R. S. & Hofmann-Goody, W. (2002). Exchange factors, effectors, GAPs and motor proteins: common thermodynamic and kinetic principles for different functions. *Eur. Biophys. J.* **31**, 268–274.
3. Grosshans, B. L., Ortiz, D. & Novick, P. (2006). Rabs and their effectors: achieving specificity in membrane traffic. *Proc. Natl Acad. Sci. USA*, **103**, 11821–11827.
4. Stenmark, H. & Olkkonen, V. M. (2001). The Rab GTPase family.*Genome Biol.* **2**; REVIEWS3007.
5. Cai, H., Reinisch, K. & Ferro-Novick, S. (2007). Coats, tethers, Rabs, and SNAREs work together to mediate the intracellular destination of a transport vesicle. *Dev. Cell*, **12**, 671–682.
6. Sacher, M., Barrowman, J., Wang, W., Horecka, J., Zhang, Y., Pypaert, M. & Ferro-Novick, S. (2001). TRAPP I implicated in the specificity of tethering in ER-to-Golgi transport. *Mol. Cell*, **7**, 433–442.
7. Cai, H., Zhang, Y., Pypaert, M., Walker, L. & Ferro-Novick, S. (2005). Mutants in trs120 disrupt traffic from the early endosome to the late Golgi. *J. Cell Biol.* **171**, 823–833.
8. Cai, H., Yu, S., Menon, S., Cai, Y., Lazarova, D., Fu, C. *et al.* (2007). TRAPPI tethers COPII vesicles by binding the coat subunit Sec23. *Nature*, **445**, 941–944.
9. Kim, Y. G., Raunser, S., Munger, C., Wagner, J., Song, Y. L., Cygler, M. *et al.* (2006). The architecture of the multisubunit TRAPP I complex suggests a model for vesicle tethering. *Cell*, **127**, 817–830.
10. Cai, Y., Chin, H. F., Lazarova, D., Menon, S., Fu, C., Cai, H. *et al.* (2008). The structural basis for activation of the Rab Ypt1p by the TRAPP membrane-tethering complexes. *Cell*, **133**, 1202–1213.
11. Esters, H., Alexandrov, K., Iakovenko, A., Ivanova, T., Thoma, N., Rybin, V. *et al.* (2001). Vps9, Rabex-5 and DSS4: proteins with weak but distinct nucleotide-exchange activities for Rab proteins. *J. Mol. Biol.* **310**, 141–156.
12. Hutchinson, J. P. & Eccleston, J. F. (2000). Mechanism of nucleotide release from Rho by the GDP dissociation stimulator protein. *Biochemistry*, **39**, 11348–11359.
13. Klebe, C., Prinz, H., Wittinghofer, A. & Goody, R. S. (1995). The kinetic mechanism of Ran–nucleotide exchange catalyzed by RCC1. *Biochemistry*, **34**, 12543–12552.
14. Guo, Z., Ahmadian, M. R. & Goody, R. S. (2005). Guanine nucleotide exchange factors operate by a

simple allosteric competitive mechanism. *Biochemistry*, **44**, 15423–15429.
15. John, J., Rensland, H., Schlichting, I., Vetter, I., Borasio, G. D., Goody, R. S. & Wittinghofer, A. (1993). Kinetic and structural analysis of the Mg(2+)-binding site of the guanine nucleotide-binding protein p21H-ras. *J. Biol. Chem.* **268**, 923–929.
16. Itzen, A., Pylypenko, O., Goody, R. S., Alexandrov, K. & Rak, A. (2006). Nucleotide exchange via local protein unfolding—structure of Rab8 in complex with MSS4. *EMBO J.* **25**, 1445–1455.
17. Itzen, A., Rak, A. & Goody, R. S. (2007). Sec2 is a highly efficient exchange factor for the Rab protein Sec4. *J. Mol. Biol.* **365**, 1359–1367.
18. Henn, A. & De La Cruz, E. M. (2005). Vertebrate myosin VIIb is a high duty ratio motor adapted for generating and maintaining tension. *J. Biol. Chem.* **280**, 39665–39676.
19. Hannemann, D. E., Cao, W., Olivares, A. O., Robblee, J. P. & De La Cruz, E. M. (2005). Magnesium, ADP, and actin binding linkage of myosin V: evidence for multiple myosin V–ADP and actomyosin V–ADP states. *Biochemistry*, **44**, 8826–8840.
20. Robblee, J. P., Olivares, A. O. & de la Cruz, E. M. (2004). Mechanism of nucleotide binding to actomyosin VI: evidence for allosteric head–head communication. *J. Biol. Chem.* **279**, 38608–38617.
21. Robblee, J. P., Cao, W., Henn, A., Hannemann, D. E. & De La Cruz, E. M. (2005). Thermodynamics of nucleotide binding to actomyosin V and VI: a positive heat capacity change accompanies strong ADP binding. *Biochemistry*, **44**, 10238–10249.
22. Henn, A., Cao, W., Hackney, D. D. & De La Cruz, E. M. (2008). The ATPase cycle mechanism of the DEAD-box rRNA helicase, DbpA. *J. Mol. Biol.* **377**, 193–205.
23. Yengo, C. M., De la Cruz, E. M., Safer, D., Ostap, E. M. & Sweeney, H. L. (2002). Kinetic characterization of the weak binding states of myosin V. *Biochemistry*, **41**, 8508–8517.
24. Bos, J. L., Rehmann, H. & Wittinghofer, A. (2007). GEFs and GAPs: critical elements in the control of small G proteins. *Cell*, **129**, 865–877.
25. Cheng, J. Q., Jiang, W. & Hackney, D. D. (1998). Interaction of mant-adenosine nucleotides and magnesium with kinesin. *Biochemistry*, **37**, 5288–5295.
26. Kinosian, H. J., Selden, L. A., Gershman, L. C. & Estes, J. E. (2000). Interdependence of profilin, cation, and nucleotide binding to vertebrate non-muscle actin. *Biochemistry*, **39**, 13176–13188.
27. Vetter, I. R. & Wittinghofer, A. (2001). The guanine nucleotide-binding switch in three dimensions. *Science*, **294**, 1299–1304.
28. Renault, L., Kuhlmann, J., Henkel, A. & Wittinghofer, A. (2001). Structural basis for guanine nucleotide exchange on Ran by the regulator of chromosome condensation (RCC1). *Cell*, **105**, 245–255.
29. Boriack-Sjodin, P. A., Margarit, S. M., Bar-Sagi, D. & Kuriyan, J. (1998). The structural basis of the activation of Ras by Sos. *Nature*, **394**, 337–343.
30. Goldberg, J. (1998). Structural basis for activation of ARF GTPase: mechanisms of guanine nucleotide exchange and GTP-myristoyl switching. *Cell*, **95**, 237–248.
31. Berg, O. G. & von Hippel, P. H. (1985). Diffusion-controlled macromolecular interactions. *Annu. Rev. Biophys. Biophys. Chem.* **14**, 131–160.
32. De La Cruz, E. M. & Pollard, T. D. (1995). Nucleotide-free actin: stabilization by sucrose and nucleotide binding kinetics. *Biochemistry*, **34**, 5452–5461.
33. Talavera, M. A. & De La Cruz, E. M. (2005). Equilibrium and kinetic analysis of nucleotide binding to the DEAD-box RNA helicase DbpA. *Biochemistry*, **44**, 959–970.
34. De La Cruz, E. M. & Pollard, T. D. (1994). Transient kinetic analysis of rhodamine phalloidin binding to actin filaments. *Biochemistry*, **33**, 14387–14392.
35. De La Cruz, E. M. & Pollard, T. D. (1996). Kinetics and thermodynamics of phalloidin binding to actin filaments from three divergent species. *Biochemistry*, **35**, 14054–14061.
36. Cao, W., Goodarzi, J. P. & De La Cruz, E. M. (2006). Energetics and kinetics of cooperative cofilin–actin filament interactions. *J. Mol. Biol.* **361**, 257–267.
37. De La Cruz, E. M., Wells, A. L., Rosenfeld, S. S., Ostap, E. M. & Sweeney, H. L. (1999). The kinetic mechanism of myosin V. *Proc. Natl Acad. Sci. USA*, **96**, 13726–13731.
38. De La Cruz, E. M., Ostap, E. M. & Sweeney, H. L. (2001). Kinetic mechanism and regulation of myosin VI. *J. Biol. Chem.* **276**, 32373–32381.
39. Vinson, V. K., De La Cruz, E. M., Higgs, H. N. & Pollard, T. D. (1998). Interactions of *Acanthamoeba* profilin with actin and nucleotides bound to actin. *Biochemistry*, **37**, 10871–10880.
40. Worthylake, D. K., Rossman, K. L. & Sondek, J. (2000). Crystal structure of Rac1 in complex with the guanine nucleotide exchange region of Tiam1. *Nature*, **408**, 682–688.
41. Zhang, B., Zhang, Y., Wang, Z. & Zheng, Y. (2000). The role of Mg^{2+} cofactor in the guanine nucleotide exchange and GTP hydrolysis reactions of Rho family GTP-binding proteins. *J. Biol. Chem.* **275**, 25299–25307.
42. Delprato, A. & Lambright, D. G. (2007). Structural basis for Rab GTPase activation by VPS9 domain exchange factors. *Nat. Struct. Mol. Biol.* **14**, 406–412.
43. Dong, G., Medkova, M., Novick, P. & Reinisch, K. M. (2007). A catalytic coiled coil: structural insights into the activation of the Rab GTPase Sec4p by Sec2p. *Mol. Cell*, **25**, 455–462.
44. Lenzen, C., Cool, R. H., Prinz, H., Kuhlmann, J. & Wittinghofer, A. (1998). Kinetic analysis by fluorescence of the interaction between Ras and the catalytic domain of the guanine nucleotide exchange factor Cdc25Mm. *Biochemistry*, **37**, 7420–7430.
45. De La Cruz, E. M. & Ostap, E. M. (2004). Relating biochemistry and function in the myosin superfamily. *Curr. Opin. Cell Biol.* **16**, 61–67.
46. Nyitrai, M. & Geeves, M. A. (2004). Adenosine diphosphate and strain sensitivity in myosin motors. *Philos. Trans. R. Soc. London Ser. B*, **359**, 1867–1877.
47. Frederick, K. B., Sept, D. & De La Cruz, E. M. (2008). Effects of solution crowding on actin polymerization reveal the energetic basis for nucleotide-dependent filament stability. *J. Mol. Biol.* **378**, 540–550.
48. Wang, W., Sacher, M. & Ferro-Novick, S. (2000). TRAPP stimulates guanine nucleotide exchange on Ypt1p. *J. Cell Biol.* **151**, 289–296.
49. John, J., Sohmen, R., Feuerstein, J., Linke, R., Wittinghofer, A. & Goody, R. S. (1990). Kinetics of interaction of nucleotides with nucleotide-free H-ras p21. *Biochemistry*, **29**, 6058–6065.
50. Alexandrov, K., Scheidig, A. J. & Goody, R. S. (2001). Fluorescence methods for monitoring interactions of Rab proteins with nucleotides, Rab escort protein, and geranylgeranyltransferase. *Methods Enzymol.* **329**, 14–31.
51. Barshop, B. A., Wrenn, R. F. & Frieden, C. (1983). Analysis of numerical methods for computer simulation of kinetic processes: development of KINSIM—a flexible, portable system. *Anal. Biochem.* **130**, 134–145.